International Journal on Interactive Design and Manufacturing (IJIDeM) (2022) 16:1705–1725
https://doi.org/10.1007/s12008-022-00964-4

ORIGINAL PAPER

Estimation of machining responses in hard turning under dry and HPC conditions using different AI based and statistical techniques

Rafat Tabassum Sukonna[1] · Prianka B. Zaman[1] · Nikhil R. Dhar[1]

Received: 8 January 2022 / Accepted: 13 June 2022 / Published online: 20 July 2022

Abstract

Hard turning is garnered as a cost-effective alternative to grinding; however, the process is marred with reliability and predictability issues. Surface roughness, cutting temperature, and cutting force are three essential elements affecting hard turning reliability. The current endeavor analyzes the machinability features of hardened medium carbon steel by measuring the performance of surface roughness, cutting temperature, and cutting force of the steel under high-pressure and dry cutting conditions using Coated carbide. An artificial neural network (ANN), response surface methodology (RSM) and adaptive neuro-fuzzy interference system (ANFIS) are utilized to model responses under two different scenarios. With a*P*-value less than 0.05, all parameters had a statistically significant effect on the output responses under dry and HPC circumstances, and the model projected values closely matched the experimental values under both situations. Several statistics show that the three output responses are effectively represented by all modeling approaches, including correlation (R), determination (R^2), mean square error (MSE), root mean square error (RMSE), and mean absolute percentage error (MAPE). As demonstrated by the correlation coefficient factor, ANFIS has a high predictive value; this indicates that the predicted response and experimental outputs have a significant consistency.

Keywords Modeling · ANFIS · ANN · RSM · Hard turning · HPC

1 Introduction

The use of hard turning to produce high-hardness steel products with acceptable machining parameters has recently gained popularity. It is also used to finish parts with a hardness of over 45 HRC to obtain error-free and precise parts. Many studies have shown that hard turning produces components with improved surface polish and dimensional precision [1]. Hard turning removes more material than grinding and reduces machining time by 60%. The high cutting zone temperature, increased tool wear and break, poor surface polish and non-optimal cutting parameters make hard turning a less attractive alternative to grinding [2].

Hardened steel is machined dry in the majority of turning operations [3]. Cutting fluids are currently being used in hard-turning processes to improve efficiency and cutting performance. High-pressure coolant (HPC) reduces cutting zone temperature, smoothes the surface, and extends tool life when turning hardened steel [4]. HPC outperformed dry and overhead fluid applications in hard-turning stainless steel with coated carbide inserts [5]. HPC lubrication appears to be a promising means of improving workpiece surface integrity and tool performance.

Bouacha et al. [6] investigated the effect of cutting parameters on surface roughness and cutting force components in hard turning of AISI 52,100 with a CBN tool using response surface methodology (RSM). The results illustrate how much feed rate and cutting speed influence surface roughness, and that the depth of cut has the greatest influence on cutting forces when compared to feed rate and cutting speed. According to ANOVA data, cutting temperature is mostly impacted by cutting speed, feed rate, depth of cut, the quadratic value of feed rate, the interaction between cutting speed and feed rate, and the interaction between cutting speed and depth of cut [7].

Coated tools, when used to transform hard materials into complex shapes and pieces, have the potential to cut manufacturing costs by up to 30 times their original value [8]. Ezugwu and colleagues [9] discussed the effect of high-pressure lubrication (HPC) on turning with coated carbide. In completed

✉ Prianka B. Zaman
prianka@ipe.buet.ac.bd

[1] Industrial and Production Engineering Department, Bangladesh University of Engineering and Technology, Dhaka 1000, Bangladesh

and extreme conditions, tool life is increased by up to 350 and 740%, respectively. In the hard machining of steels, both coated and uncoated carbide tools are widely used. After testing the performance of uncoated carbide and coated carbide tools on hardened steel turning, Das and colleagues [10] discovered that coated carbide tools performed significantly better than uncoated carbide tools. Coating technology advancements have allowed for the development of coated carbide tools with qualities such as hardness, high toughness values, enhanced fracturing strength, wear resistant capabilities, and improved thermal shock resistance. Coating materials have high wear resistance and are chemically inert, which protects the tool and workpiece from chemical interaction during the machining process [11].

Surface roughness is an important factor in product production and has a substantial impact on [12] machining costs when turning. A piece of work's surface finish is affected by cutting factors such as cutting speed, feed rate, and depth of cut**.** High-pressure coolant application is a viable method for increasing surface smoothness [13]**.** During hard turning, several reasons are thought to be responsible for the challenges, with cutting temperature being the most significant. Another study found that HPC reduces cutting temperature, chip-tool interface temperature, tool wear, and increases surface smoothness [4]**.** Cutting forces can help explain the machining process because they are directly related to cutting conditions and tool conditions. HPC also reduces cutting forces during hard turning compared to dry machining [14]**.**

Modeling and optimization methods in metal cutting are critical in today's rapidly expanding industrial sector since they reduce tooling, production, and maintenance costs while simultaneously increasing total productivity. While the predictive model sets the equation connecting input and output to define the machining process's objective function, the optimization approach offers an optimal or near-optimal solution(s) for the stated objective function that the production engineer can execute on the shop floor. Among the several artificial intelligence-based soft computing systems, the artificial neural network (ANN) has been extensively used in machining operations because of its superior prediction accuracy. Sharma et al. [15] developed an ANN model of surface roughness in terms of speed, feed rate, depth of cut, and approaching angle for hard turning and discovered a 76.4% accuracy. ANN is regarded as a highly effective empirical technique since it considers the non-linear relationship between the process's input and output parameters (performance characteristics). Additionally, neural networks with a single output fared better than neural networks with two outputs combined [16].

Another modeling and optimization method is RSM, which is used to acquire the levels of machining parameters that are required to achieve the desired level of responsiveness in a given situation. The RSM model produced excellent results in terms of forecasting cutting temperature and surface roughness [7, 17]. Surface roughness forecasts were accurately predicted by the ANN model, which generally exhibited better overall performance, especially when compared to the conventional RSM model [18]. In a recent work ANN model was also found effective than RSM model in predicting surface roughness and cutting force components under dry conditions [19].It was also found in another article that ANN outperformed RSM when it came to forecasting cutting temperature in HPC [20]. ANN was also found to be more accurate than RSM in predicting cutting forces in a separate study [21]. Sometimes, nevertheless, it was found that the RSM model was a better way to predict surface roughness than ANN [22]. Another artificial intelligence tool, the adaptive neural fuzzy inference system (ANFIS), enables the industrial business to grow positively [23]. ANFIS is a strong modeling technique that is based on a fuzzy inference system and a neural network. It is used to describe complicated interactions in numerous fields of industry and engineering that are difficult or impossible to explain using classical models [24]. This artificial intelligence technique has been effectively used in the modeling of a variety of machining processes, including turning, milling, and drilling [25, 26]. In another recent study, the ANFIS model was found to be very reliable in predicting cutting temperature with very little error [27]. However, in another study, ANFIS outperformed ANN in terms of obtaining cutting force components, tool wear, and surface roughness during HPC [28]. In addition, the ANFIS Model was found to be more reliable than the RSM Model in forecasting flank wear and surface roughness under dry conditions [29].

A systematic comparison has been performed between the three contemporary ML and statistical model. As there have been no systematic comparison between these three popular models on the same data in hard turning process under dry and HPC condition, this study will help in the decision making and choosing the best model in real life scenarios. Although it can be seen from the literature review that numerous predictive models have been developed to study the impact of variables (cutting speed, feed rate, depth of cut) on responses and, certain experimental research into the capabilities of high-pressure cooling (HPC) was carried out; to the best of our knowledge, no such research has been conducted employing ANN, ANFIS, and RSM models under HPC for predicting machining performances. The goal of this study is to get a better knowledge of surface roughness, cutting temperature, and cutting force during the hard turning of medium carbon steel under the impact of HPC and Dry. The objective of this study is to find the optimum model for predicting surface roughness, cutting temperature, and cutting force in the hard turning process, which will help to reduce costs and boost productivity.

Table 1 Experimental conditions

Machine tool		Centre lathe 10 hp (China)
Work material		Hardened Medium Carbon Steel, AISI 1045
	Composition	C = 0.420–0.50%, Fe = 98.51–98.98%, Mn = 0.60–0.90%, P ≤ 0.040% and S ≤ 0.050%
	Size	External dia. = 87 mm, Internal dia. = 48 mm and L = 230 mm
	Hardness (HRC)	56
Tool holder		PSBNR 2525 M 12 (WIDIA)
Cutting tool insert		Coated carbide (SNMG 120,408 TN 4000)
Working tool geometry		− 6°, − 6°, 6°, 15°, 75° and 0.8 mm
Process parameters		
	Cutting speed (V)	96 ~ 174, m/min
	Feed (f)	0.10 ~ 0.14 mm/rev
	Depth of cut (d)	0.2 ~ 0.6 mm
Machining Environment		High-pressure coolant (HPC)
HPC supply properties		
	Coolant type	HC Straight run, VG 68
	Pressure	70 bar
	Flow rate	4 L/min through an external nozzle having 0.5 mm tip diameter

2 Machine, material, methodology

Under high-pressure coolant conditions, the experiment was executed at a variety of industrial feed rates (f), cutting speeds (V), and for a variety of cut depths. With the help of a sturdy and solid lathe with a capacity of 10 horsepower and a maximum spindle speed of 1400 rpm, the machining trials were carried out. The experimental strategy involved hard turning of hardened steel in dry and high-pressure coolant environments. The cutting speed, V (96, 135, and 174 m/min), and feed rate, f (0.1, 0.12 and 0.14 mm/rev) ranges were chosen based on tool manufacturer recommendations and industrial practices. For the finishing operation of the studied tool-work-piece combination, the suggested depth of cut range is 0.3 mm to 2 mm (Widia TM Value). Taking this into account, the d value was selected to (0.2, 0.4 and 0.6 mm) [30]. Table 1 shows the current experimental conditions, which are as follows:

To satisfy the criteria of the current research activity, which include an uninterrupted supply of coolant at a pressure of approximately 70 bar over a reasonably long cut, a coolant tank was used. The experimental setup is photographed in conjunction with the high-pressure coolant system, which consists of the motor-pump assembly, relief valve, flow control valve, and directional control valve. Cutting fluid must be drawn from the coolant tank, pressurized to high pressure with a vane pump, and then rapidly intruded through the nozzle. A high-pressure coolant jet is directed at an angle through a nozzle from an appropriate distance away from the chip-tool interface, and it is focused on such a way that it reaches the rake and flank surfaces and shields the auxiliary flank, enhancing dimensional precision. The experimental setup is shown in Fig. 1(a).

After each cut, the surface roughness of the machined surface was determined using a Talysurf (Surtronic 3+) with a sampling length of 0.8 mm. The average cutting temperature in high-pressure coolant conditions was determined using a reliable tool-work thermocouple approach with suitable calibration [30]. The view of calibration set up and temperature calibration graph are shown in Fig. 1(b). A dynamometer (Kistler) was used to measure the main cutting force (Fc) during hard turning at various V-f-d combinations under high-pressure coolant conditions. Charge amplifiers were used to amplify the charge signal generated by the dynamometer (Kistler). A computer-based data acquisition system is used to acquire and sample the amplified signal at a sampling rate of 2000 Hz per channel. The time-series profiles of the collected force data indicate that the forces are reasonably constant throughout the length of the cut and that effects such as vibration and spindle run-out are minimal. Table 2 shows different process inputs with their levels and Table 3 shows the experimental responses for all the experimental run.

2.1 Predictive models

2.1.1 Artificial neural network model

Nowadays, artificial neural networks are acknowledged as one of the most robust nonlinear mapping systems, capable of solving a wide variety of problems such as optimization,

(a) Photographic view of the experimental set up

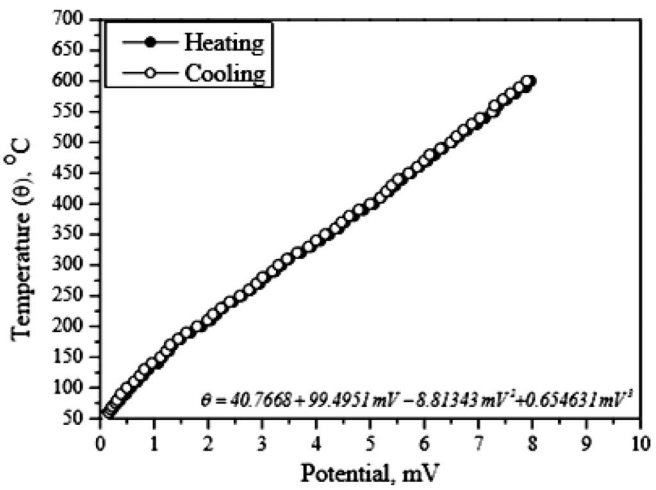

(b) Photographic view of the calibration set-up and temperature calibration curve for carbide and hardened medium carbon steel

Fig. 1 **a** Photographic view of the experimental set up, **b** Photographic view of the calibration set-up and temperature calibration curve for carbide and hardened medium carbon steel

Table 2 Factors and levels used in the experimental plan

Level	Cutting speed(m/min)	Depth of cut(mm)	Feed rate(mm/rev)	Cutting condition
1	96	0.2	0.1	Dry
2	135	0.4	0.12	HPC
3	174	0.6	0.14	–

Table 3 Experimental data

Exp. No	Cutting speed (m/min)	Feed rate (mm/rev)	Depth of cut (mm)	Cutting condition	Surface roughness (Ra)	Cutting temperature (T)	Cutting force (F)
1	135	0.12	0.4	HPC	0.85	892	188
2	135	0.14	0.2	HPC	0.86	892	162
3	135	0.12	0.4	HPC	0.88	898	189
4	174	0.14	0.4	HPC	0.89	923	210
5	174	0.1	0.4	HPC	0.68	898	148
6	96	0.12	0.6	HPC	1.03	911	266
7	96	0.14	0.4	HPC	1.12	898	274
8	174	0.12	0.2	HPC	0.71	892	129
9	135	0.1	0.6	HPC	0.81	936	219
10	174	0.12	0.6	HPC	0.85	911	223
11	135	0.12	0.4	HPC	0.86	898	188
12	96	0.12	0.2	HPC	0.81	866	154
13	135	0.14	0.6	HPC	1.1	923	308
14	135	0.1	0.2	HPC	0.69	848	111
15	96	0.1	0.4	HPC	0.81	873	186
16	135	0.12	0.4	HPC	0.85	904	187
17	135	0.12	0.4	HPC	0.83	892	188
18	135	0.12	0.4	Dry	1	967	238
19	135	0.14	0.2	Dry	1.01	980	175
20	135	0.12	0.4	Dry	1.06	974	237
21	174	0.14	0.4	Dry	1.12	992	253
22	135	0.1	0.6	Dry	0.98	948	267
23	135	0.14	0.6	Dry	1.35	999	389
24	96	0.12	0.2	Dry	1.06	936	170
25	174	0.12	0.2	Dry	0.78	967	135
26	135	0.12	0.4	Dry	0.99	961	237
27	174	0.1	0.4	Dry	0.77	955	188
28	135	0.1	0.2	Dry	0.72	923	133
29	174	0.12	0.6	Dry	1.06	980	305
30	96	0.14	0.4	Dry	1.28	974	292
31	96	0.1	0.4	Dry	0.96	917	220
32	135	0.12	0.4	Dry	1	967	237
33	96	0.12	0.6	Dry	1.18	974	330
34	135	0.12	0.4	Dry	0.97	967	236

pattern recognition, control, time series modeling, and function approximation, among others. For modeling complex nonlinear relationships, ANN can be used in place of polynomial regression and produces more precise results [31]. To augment existing data analysis technologies, ANNs are recognized as one of the simplest mathematical models [32], consisting of three interconnected layers with one or more neurons in each layer. The first layer is referred to as the input layer, and it is where the model gets numerical data as input. At this point, a neuron is regarded as a single variable. The second layer is referred to as the hidden layer; it receives data from the input layer and processes it further. The third layer, named the Output layer, is coupled to the hidden layer via synaptic weights and gives an output (s). The precision of an ANN model is determined by the configuration, the various functions, the training algorithm, and the weights and biases. The primary disadvantage of building an ANN model is selecting the ideal number of neurons to achieve the most accurate outcome feasible.

For predicting machining performances under HPC and dry, this research utilized the most well-known and well-established technique, a feed forward error back-propagation training algorithm of ANN. The algorithm has a '3-n-1' architecture and is used to predict cutting forces, temperature, and surface roughness in the hard turning operation, and the feed-forward back propagation algorithm yielded the most error-free results [33]. Using the 'nnstart' wizard, MATLAB R2020a has been utilized to create, train, and test the neural network. Neural networks have been developed by using a tangent of the sigmoid activation function in the hidden layer and in the output layer because of their symmetric nature [34].

2.1.2 Response surface methodology

The response surface methodology is a synthesis of numerous mathematical and statistical techniques that enables us to optimize, develop, and improve a wide variety of processes [35]**.** RSM is a statistical and mathematical technique that generates a unique relationship between dependent and independent variables, as well as mathematical connections [36]. This model makes it simple to determine the effects of process variables on output response, and its prediction and optimization capabilities are also rather good. Additionally, as shown in Eq. (1) and (2), the RSM model can be used to construct both linear and quadratic models (2).

$$X = \beta_0 + \beta_1 x_1 + \beta_2 x_2 + \beta_3 x_3 + \ldots\ldots\ldots\ldots\ldots\ldots\ldots\ldots\ldots\ldots + \beta_n x_n + \xi \quad (1)$$

$$X = \beta_0 + \sum_{(i=1)}^{k} \beta_i x_i + \sum_{(i=1)}^{k} \beta_{ii} x^2 + \sum \sum_{(i<j)} \beta_{ij} x_i x_j + \xi \quad (2)$$

Here X is the response parameter– cutting temperature, surface roughness, and cutting force; In Eq. (1) β_0 is the fixed term while linear coefficient terms are β_1; β_2 …..; in Eq. (2) the coefficients of linear, quadratic, and cross-product terms are β_i, β_{ii}, β_{ij} respectively; x_i is the input variables (i.e. cutting speed, feed rate and depth of cut).

CCD (Central Composite design) and BBD (Box-Behnken design) are the two most frequently used designs for optimizing multiple responses in hard turning operations. Box and Behnken first proposed RSM factorial designs (BBD) with three-level factors to fit quadratic models to the responses [37].In this research, the BBD of the RSM approach was applied for the conduct of the experiment.

2.1.3 Adaptive neuro-fuzzy inference system

For diverse applications, an adaptive neuro-fuzzy inference system is a fusion intelligent computing approach that integrates ANN with a fuzzy system. [37, 38]. Jang was the first to launch it in 1993 [39]. This network has a five-layered hybrid system with various functions, as shown below.

Layer I (Fuzzy layer): This ANFIS layer turns a collection of inputs to a fuzzy set by the use of a membership function. The adaptive nodes in this layer perform the following functions:

$$\begin{aligned} &Z1,\ i\ =\ \mu Pi(M)(i = 1, 2) \\ &Z1,\ j\ =\ \mu Qj(N)(j\ = 1, 2)(2)\ Z1,\ k\ =\ \mu Rk(\ O)\ (k = 1, 2) \end{aligned} \quad (3)$$

Here input variable nodes M, N, and O are with i, j, k, P, Q, and R are the labels associated with the input node. μ(M), μ(N), and μ(O) are considered as membership functions and because of versatility Gaussian shape membership function was selected.

Layer II(product layer (π)): The output signal is obtained by multiplying the input signal by the node function and the nodes are fixed in this layer.

$$Z2,\ i = Wi\ = \mu Pi(M).\mu Qj(N).\mu Rk(O),\ (\ \text{for i};\ \text{j and k}\ = 1, 2) \quad (4)$$

where Z2, i represents the output of layer II and the strength of fuzzy rule setup is Wi.

Layer III (normalized layer (N)): This layer computes the normalized firing strength of a rule acquired from the preceding layer, as well as a, has fixed node network whose strength is expressed as:

$$Z3,\ i = Wx = \frac{Wi}{(W1\ +\ W2)},\ (for\ i = 1, 2) \quad (5)$$

Here the output of layer III is Z3, i, and Wx is the normalized strength rule.

Layer IV(defuzzy layer): Each node represents a section of the fuzzy rule that is consistent, and nodes can be adjusted in this layer.

$$Z4,\ i = Wxi.fi,\ (for\ i = 1, 2) \quad (6)$$

where the normalized weighting factor of the ith rule is Wxi- and fi is a fuzzy rule for i = 1, 2 so fuzzy rule for a system is given as:

$$fi = (Pix1 + Qix2 + Ri)$$

andPi, Qi, and Ri are the set parameters.

Layer V(Total output layer): Defuzzification of the subsequent part of the rule is achieved in this layer by adding the outputs of all the rules.

$$Z5,\ i\ =\ \Sigma iWni.fi,\ (\text{for i} = 1,\ 2) \tag{7}$$

Here Z5, i is the output of this layer.

ANFIS system has several advantages over traditional estimating methods, the most significant of which is that it does not require any changes to the existing model structure. It is possible to simply supplement the model with new input parameters, as well as to automatically explore the non-linear relationship between the input parameters (cutting speed, depth of cut, feed rate) and the output parameters (surface roughness, cutting temperature, cutting force).

2.2 Comparison parameters

The significance of the ANFIS, ANN and RSM models were evaluated concerning different statistical parameters like the coefficient of correlation (R), coefficient of determination (R^2), mean square error (MSE), root mean square error (RMSE), mean absolute error (MAPE). The representing equations Eqs. (8), (9), (10), (11), (12) of these parameters are given below

$$R = \frac{\sum_1^n (x-\overline{x})(y-\overline{y})}{\sqrt{\sum_1^n (x-\overline{x})^2 \sum_1^n (y-\overline{y})^2}} \tag{8}$$

$$R2 = \left(\frac{\sum_1^n (x-\overline{x})(y-\overline{y})}{\sqrt{\sum_1^n (x-\overline{x})^2 \sum_1^n (y-\overline{y})^2}}\right)^2 \tag{9}$$

$$MSE = \frac{\sum_1^n (y-x)^2}{n} \tag{10}$$

$$RMSE = \sqrt{\frac{\sum_1^n (y-x)^2}{n}} \tag{11}$$

$$MAPE = \frac{1}{N}\sum_{i=1}^{n} \frac{|Actual - predicted|}{Actual} \times 100 \tag{12}$$

3 Result and discussion

3.1 ANN model

The back-propagation technique was employed as the learning algorithm in this modeling method. The Bayesian regularization technique termed 'trainbr' by MacKay [40] can be used to overcome difficulties associated with imprecise noisy input and over-or under-fitting in neural network training. So, the Bayesian regularization algorithm called 'trainbr' was chosen as the training algorithm in this modeling method. The hyperbolic tangent sigmoid function 'tansig' was used as the transfer function for the hidden and output layers, respectively, during modeling. It is worth noting that the 'tansig' was chosen for its symmetrical character [34].

To identify the ideal architecture, we created and tested many networks with varying layers and neurons in the hidden layer. Using a trial and error strategy to determine the most accurate model is one of the most effective methods for ANN model training, especially when a hybrid model such as an ANN-genetic model is not utilized [41]. As a result, the number of neurons in the hidden layer was calculated statistically. The applied technique for determining the ANN model with the lowest error in predicting surface roughness under HPC is illustrated in Fig-2. The ANN model with three inputs (cutting speed, depth of cut, and feed rate), one hidden layer, 14 neurons in the hidden layer, and one output performed the best at predicting surface roughness under HPC. As illustrated in Fig. 2, we can see that when three outputs are predicted simultaneously, the model's accuracy declines.

Table 4 detail various ANN models for three distinct output responses and their associated RMSE. The number of hidden layers were varied starting from a base point of 6 hidden layers. As can be seen from Fig. 2 the RMSE value started to decrease after 8 hidden layers; however, the RMSE value started to increase after 20 hidden layers. Increasing the number of steps did not improve the results either. The optimal ANN structure for surface roughness under HPC is 3-14-1 based on the lowest RMSE value, but the RMSE was high when we applied the same structure for other responses. As a result, different responses based on a trial-and-error technique resulted in diverse ANN structures. Actual and anticipated data were compared to determine the adequacy of the ANN models and in all cases, predicted values were found to be close to observed values, showing that the data were well-fitted. The R, R^2, MAPE, MSE, RMSE between the simulated and experimental data for surface roughness, cutting temperature, and cutting force under HPC and Dry conditions are shown in Tables 7, 8. The R-values for various responses under various conditions are depicted in Fig. 3.

3.2 RSM model

According to the BBD, the investigation was carried out to investigate the effect of factors (cutting speed, depth of cut, and feed rate) on surface roughness, cutting temperature, and cutting force in HPC and dry cutting conditions using Design-Expert13 software. Different linear and quadratic equations were created by expressing the responses concerning three input factors using experimental results.

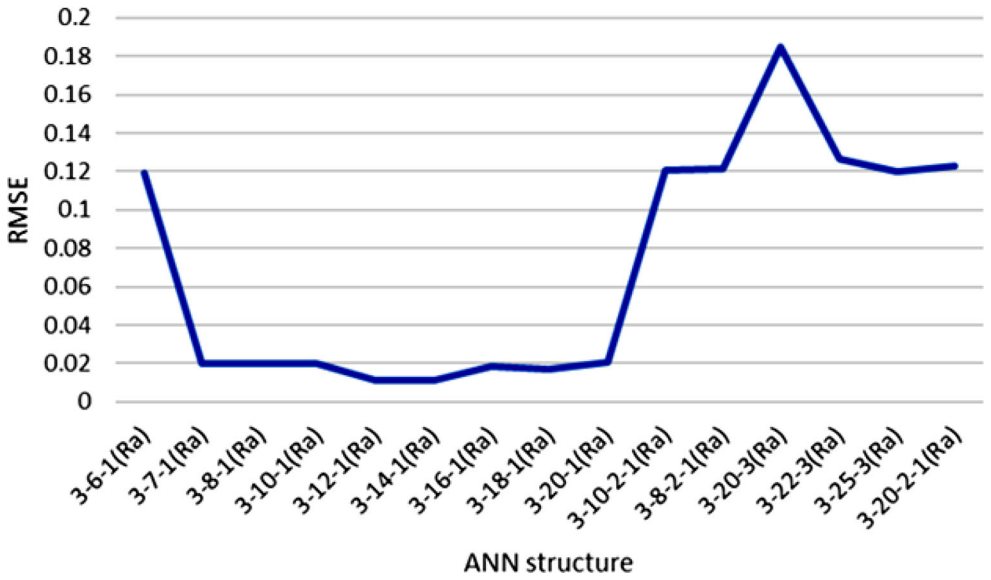

Fig. 2 The error of the ANN models in predicting the Ra in terms of the number of neurons and hidden layer

Table 4 Optimum ANN model and corresponding lowest RMSE

Responses Under dry	ANN-Structure	Lowest RMSE	Responses Under HPC	ANN-Structure	Lowest RMSE
Surface Roughness (μm)	3-10-1	0.022331316	Surface Roughness (μm)	3-14-1	0.010942127
Cutting force (N)	3-6-1	1.451414615	Cutting force (N)	3-8-1	0.452207264
Cutting temperature (˚C)	3-18-1	1.451414615	Cutting temperature (˚C)	3-3-2-1	4.121278679

The RSM model equations, Eq. 13–18 are expressed in terms of coded factors below.

$$(\textbf{Surface Roughness})_{\textbf{HPC}} = 0.86 - 0.080A + 0.090B + 0.12C - 0.020AB - 0.025AC + 0.030BC \quad (13)$$

$$(\textbf{Surface Roughness})_{\textbf{Dry}} = 1.02 - 0.094A + 0.13B + 0.17C \quad (14)$$

$$(\textbf{Cutting Force})_{\textbf{HPC}} = 195.88 - 21.25A + 57.50B + 36.25C \quad (15)$$

$$(\textbf{Cutting Force})_{\textbf{Dry}} = 237.76 - 16.38A + 84.75B + 37.63C + 2.50AB - 1.75AC + 20.00BC \quad (16)$$

$$(\textbf{Cutting Temperature})_{\textbf{HPC}} = 897.35 + 9.50A + 22.88B + 10.12C - 6.50AB + 0.000AC - 14.25BC \quad (17)$$

$$(\textbf{Cutting Temperature})_{\textbf{HPC}} = 963.59 + 11.63A + 11.87B + 25.25C \quad (18)$$

hereA = Cutting Speed, B = Depth of cut and C = Feed rate.

The analysis of variance (ANOVA) is used to assess the impact of several variables on the dependent variable (surface roughness, cutting temperature, and cutting force shown in Table 5. The ANOVA table contains the sequential sum of squares, from which the percentage contribution of factors is calculated, as well as the F-value and *P*-value. The *P*-value reflects the significance of a factor at a 95% confidence level. The higher the F-value, the greater the relevance of that factor.

Cutting speed, feed rate, and depth of cut are all statistically significant for RSM surface roughness, cutting force, and cutting temperature models, as the *P*-values are less than 0.05. The important interactions for the surface roughness model under dry cutting conditions are depth of cut-feed rate and feed rate speed. The depth of cut-feed rate is the sole relevant interaction term for the cutting force model under dry and cutting temperature under HPC.

Figure 4 depicts the regression curve of actual and expected surface roughness, cutting force, and cutting temperature for the RSM model. The regression coefficient values for three output response models are shown in Table 7, and these results indicate that the model is appropriate for predicting surface roughness, cutting force, and cutting temperature in both machining conditions. Because of the larger

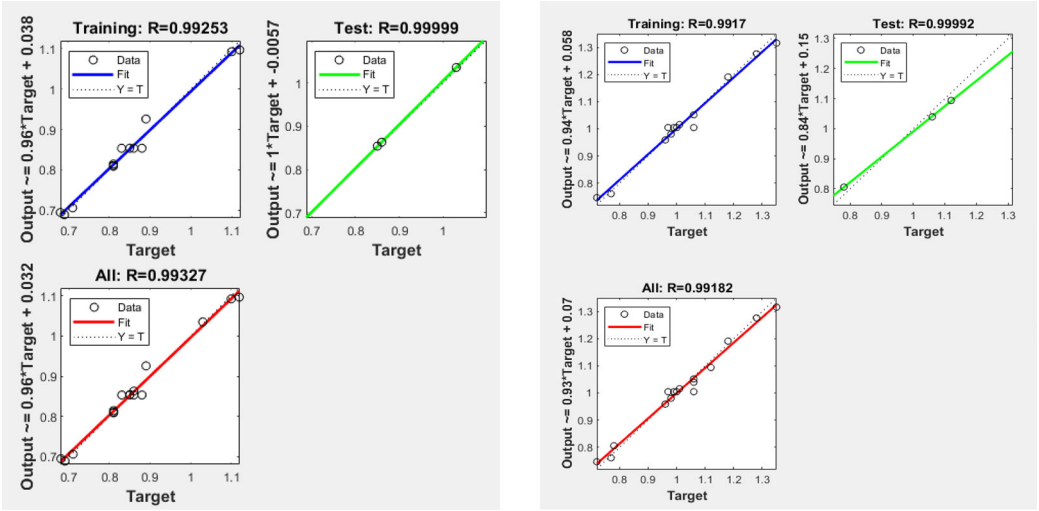

(a) **(b)**

Actual vs Predicted surface roughness (Ra) under (a) HPC and (b) Dry

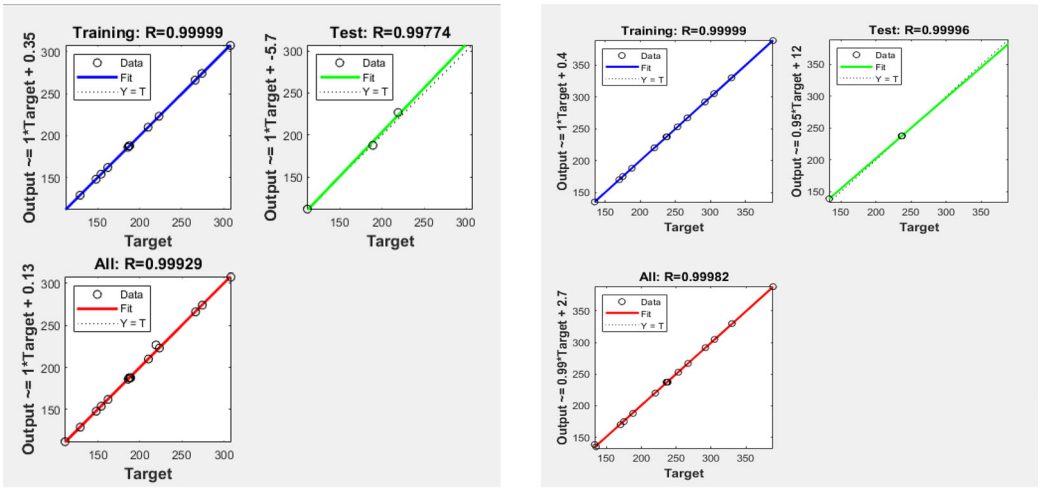

(c) **(d)**

Actual vs Predicted cutting force (F) under (c) HPC and (d) Dry

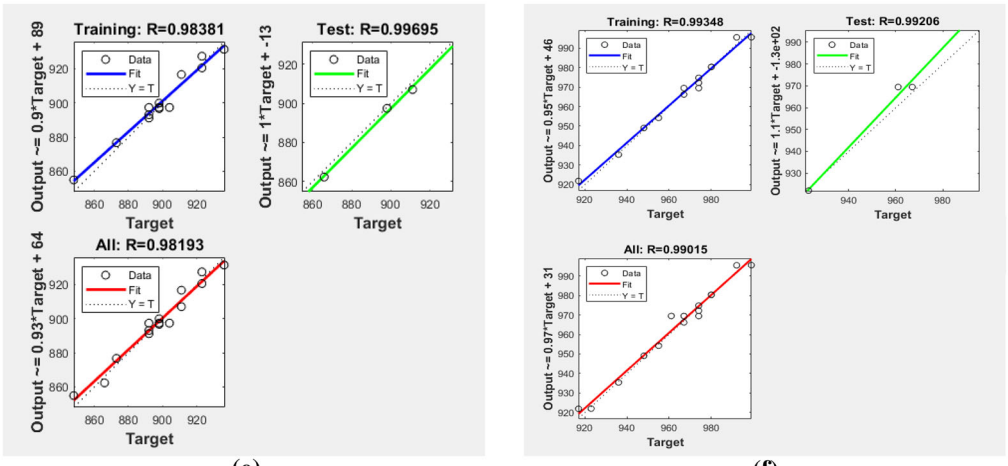

(e) **(f)**

Actual vs Predicted cutting temperature (T) under (c) HPC and (d) Dry

Fig. 3 Actual vs Predicted surface roughness (Ra) under **a** HPC and **b** Dry, Actual vs Predicted cutting force (F) under **c** HPC and **d** Dry Actual vs Predicted cutting temperature (T) under **e** HPC and **f** Dry

Table 5 **a** ANOVA table for surface roughness under HPC and Dry **b** ANOVA table for Cutting force under HPC and Dry **c** ANOVA table for Cutting temperature under HPC and Dry

		Response 1-Surface roughness under HPC				Response 2-Surface roughness under Dry			
		ANOVA for Response surface 2FI Model				ANOVA for Response surface Linear Model			
(a)									
Source		Ss	df	F- value	p-value	Ss	df	F- value	p-value
Model		0.24	6	98.03	< 0.0001	0.42	3	90.55	< 0.0001
A-Cutting Speed		0.051	1	123.55	< 0.0001	0.07	1	45.87	< 0.0001
B-Depth of Cut		0.065	1	156.37	< 0.0001	0.13	1	81.54	< 0.0001
C-Feed rate		0.12	1	289.69	< 0.0001	0.22	1	144.24	< 0.0001
AB		1.60E − 03	1	3.86	0.0778	–	–	–	–
AC		2.50E − 03	1	6.03	0.0339	–	–	–	–
BC		3.60E − 03	1	8.69	0.0146	–	–	–	–
Residual		4.14E − 03	10	1.43	0.3811	0.02	13	–	–
	Lack of Fit	2.82E − 03	6	1.43	0.3811	0.015	9	1.52	0.365
	Pure Error	1.32E − 03	4	–	–	4.52E-03	4	–	–
Cor Total		0.25	16	–	–	0.44	16	–	–
		Response 3-utting force under HPC				Response 4-Cutting force under Dry			
		ANOVA for Response surface linear Model				ANOVA for Response surface Linear Model			
(b)									
Source		Ss	*df*	F-value	*p*-value	Ss	*df*	F- value	*p*-value
Model		40,575	3	99.52	< 0.0001	72,568	6	537.4	< 0.0001
A-Cutting Speed		3612.5	1	26.58	0.0002	2145.13	1	95.31	< 0.0001
B-Depth of Cut		26,450	1	194.62	< 0.0001	57,460.5	1	2553.13	< 0.0001
C-Feed rate		10,512.5	1	77.35	< 0.0001	11,325.13	1	503.21	< 0.0001
AB		–	–	–	–	25	1	1.11	0.3167
AC		–	–	–	–	12.25	1	0.54	0.4776
BC		–	–	–	–	1600	1	71.09	< 0.0001
Residual		1766.76	13	–	–	225.06	10	–	–
	Lack of fit	1764.76	9	392.17	< 0.0001	223.06	6	74.35	0.0005
	Pure error	2.00E + 00	4	–	–	2	4	–	–
Cor. total		42,341.76	16	–	–	72793.06	16	–	–
		Response 5-Cutting temperature under HPC				Response 6-Cutting temperature under Dry			
		ANOVA for response surface 2FI model				ANOVA for response surface linear model			
(c)									
Source		Ss	*df*	F-value	*p*-value	Ss	*df*	F- value	*p*-value
Model		6709.5	6	17.35	< 0.0001	7309.8	3	56.13	< 0.0001
A-Cutting speed		722	1	11.2	0.0074	1081.1	1	24.9	0.0002
B-Depth of cut		4186.13	1	64.96	< 0.0001	1128.1	1	25.99	0.0002
C-Feed rate		820.12	1	12.73	0.0051	5100.5	1	117.49	< 0.0001
AB		169	1	2.62	0.1364	–	–	–	–

Table 5 (continued)

		Response 5-Cutting temperature under HPC				Response 6-Cutting temperature under Dry			
		ANOVA for response surface 2FI model				ANOVA for response surface linear model			
AC		0	1	0	1	–	–	–	–
BC		812.25	1	12.61	0.0053	–	–	–	–
Residual		644.38	10	–	–	564.37	13	–	–
	Lack of fit	543.58	6	3.6	0.118	479.57	9	2.51	0.1944
	Pure error	100.8	4	–	–	84.8	4	–	–
Cor total		7353.88	16	–	–	7874.1	16	–	–

F-value, the feed rate is the most critical factor in surface roughness and cutting temperature in dry cutting conditions. Similarly, the depth of cut for cutting force and cutting temperature contribute the most under HPC.

The three-dimensional response surface plots of surface roughness under HPC are shown in Fig. 5. Figure 5(a) depicts the relationship of surface roughness with feed rate and cutting speed, whereas Fig. 5(b) depicts the relationship with cutting speed and depth of cut, and Fig. 5(c) feed rate-depth of cut. Low surface roughness is associated with low feed rate, depth of cut, and high cutting speed in dry and HPC cutting, whereas high surface roughness is associated with high feed rate, depth of cut, and low cutting speed. The high-pressure coolant lowers surface roughness in all circumstances. Similarly, in dry and HPC cutting, low feed rate, depth of cut, and cutting speed are associated with low cutting temperature, while the high cutting temperature is generated at high feed rate, depth of cut, and cutting speed, and HPC creates more cutting temperature than dry cutting circumstances. In dry and HPC cutting conditions, low feed rate, depth of cut and higher cutting speed is associated with low cutting force, whereas high force is created at low feed rate, depth of cut, and lower cutting speed, and HPC also reduces cutting force during machining operation when compared to dry cutting condition**.**

3.3 ANFIS model

This section explains how the experimental data and the ANFIS model output differ based on the machining parameters. Table 6 shows the ANFIS output values for surface roughness, cutting temperature, and cutting force under HPC and dry cutting conditions.

The suggested ANFIS model for surface roughness, cutting force, and cutting temperature under both cutting conditions with three input parameters and one output parameter comprises the approach below to predict the process output parameters.

- In the command window, enter all of the input values and their corresponding output responses, and then load everything into the ANFIS editor toolbox, which is primarily based on the Sugeno fuzzy model, as shown in Fig. 6.
- The fuzzy inference system is then created using the grid partitioned technique.
- In most cases, the proposed fuzzy set's membership function can be parameterized membership function.
- A total of 1000 epochs are used to train the model. The input and output parameters are modified during the training process, and the error is minimized for each epoch. Figure 7depicts the error minimization process.
- The data was then tested using fuzzy inference systems that adapt their rules in a self-manner and predicted surface roughness values using ANFIS.

In all cases, R values greater than 0.9 suggest a strong link between the actual and anticipated values; the created ANN models, which were trained using actual values, accurately predicted the responses [42]**.**The adaptive neuro-fuzzy interference system performs well in terms of coefficient of correlation, coefficient of determination (R^2), MSE, MAPE, and RMSE for all three outputs. The coefficient of determination reflects how much of the variance between the two variables is explained by the linear fit and it is shown in Fig. 8. The value of the Correlation coefficient (R) for surface roughness under HPC is 0.9973, indicating that 99.73 percent of the variance is predictable. Tables 7, 8 displays all of the correlation coefficients and related RMSE and MAE. All of the correlation coefficients are close to one, indicating that the variables are positively linearly connected and that the scatter plot follows virtually a straight line with a positive slope.

3.4 Comparative analysis of ANN, RSM and ANFIS models

The ANFIS, ANN, and RSM techniques were used in this study to predict surface roughness, cutting force, and cutting

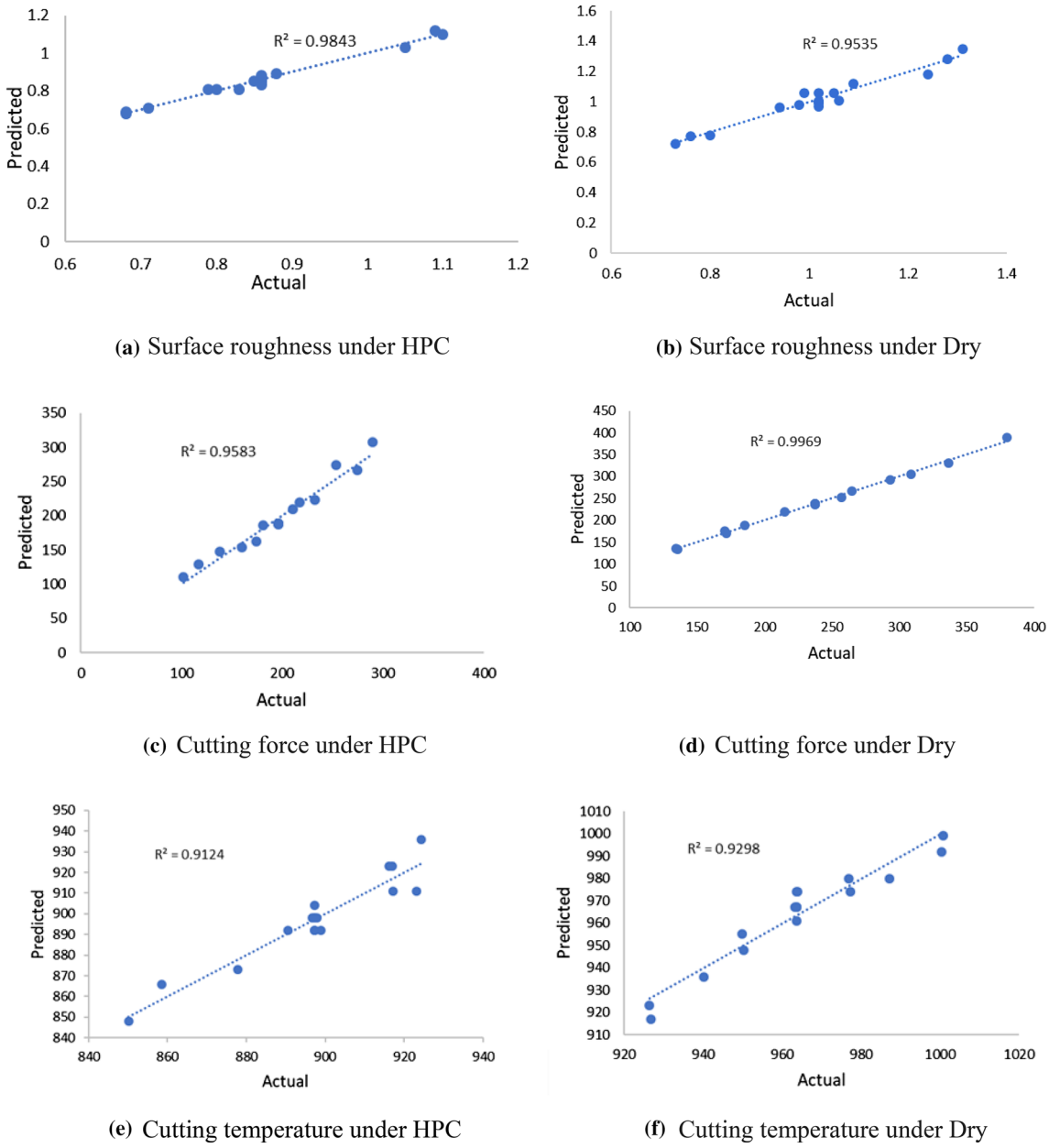

(a) Surface roughness under HPC

(b) Surface roughness under Dry

(c) Cutting force under HPC

(d) Cutting force under Dry

(e) Cutting temperature under HPC

(f) Cutting temperature under Dry

Fig. 4 **a** Surface roughness under HPC **b** Surface roughness under Dry **c** Cutting force under HPC **d** Cutting force under Dry **e** Cutting temperature under HPC **f** Cutting temperature under Dry

temperature under HPC and Dry cutting circumstances. The predictive models created by ANFIS, RSM and ANN were compared based on their prediction accuracy as measured by their coefficient of determination (R2), coefficients of correlation (R), Mean absolute error (MAE) and root mean square error (RMSE) shown in Table 7, 8. The good relationship between the input values demonstrated that the models built are suitable for simulating actual results. To assess the accuracy of the constructed ANFIS, ANN and RSM models, the predicted data were compared with the actual data, as shown in Fig. 9. The values were plotted against the run numbers of the experiment. The results reveal that the model projected values for surface roughness, cutting force, and cutting temperature under HPC and Dry cutting circumstances were in close agreement with the corresponding experimental values in all three approaches. However, ANFIS models were found to be marginally more accurate in predicting responses than ANN and RSM.

The R^2 computed by ANFIS was more accurate as the values were closer to one than the ANN and RSM techniques. This means that the models produced by ANFIS were more

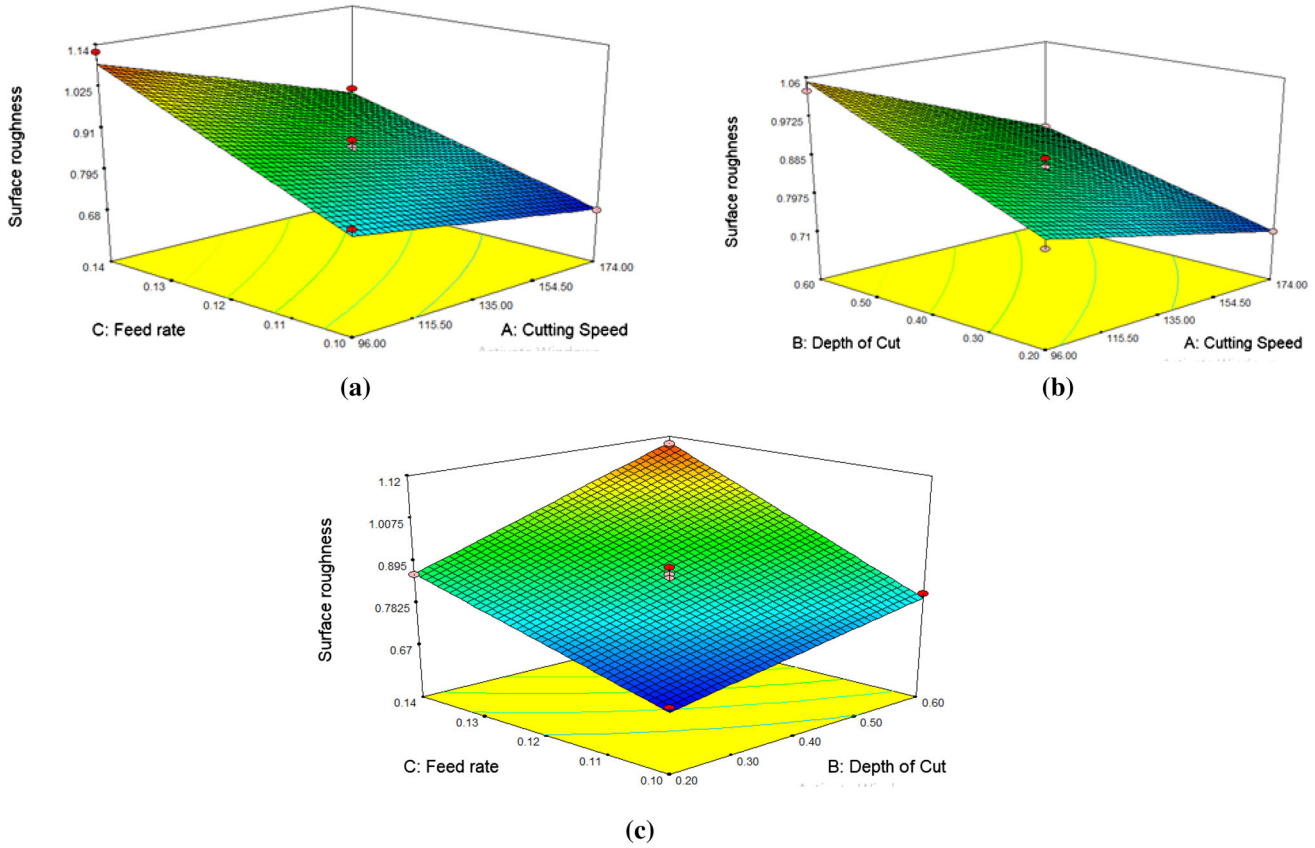

Fig. 5 Response Surface plot of Surface roughness under HPC

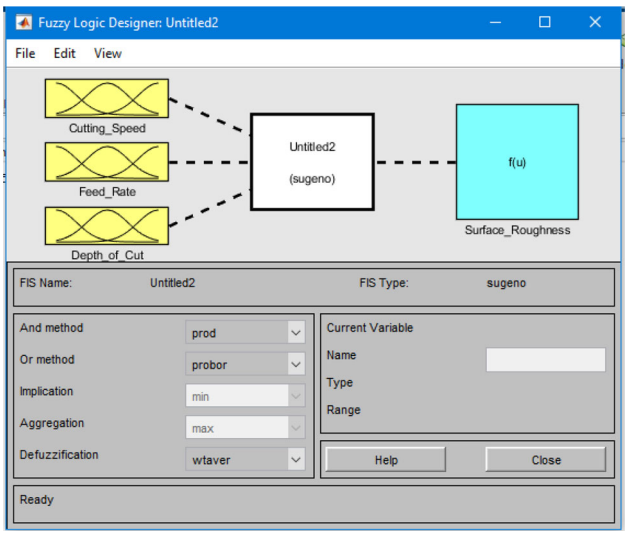

Fig. 6 Command window of ANFIS

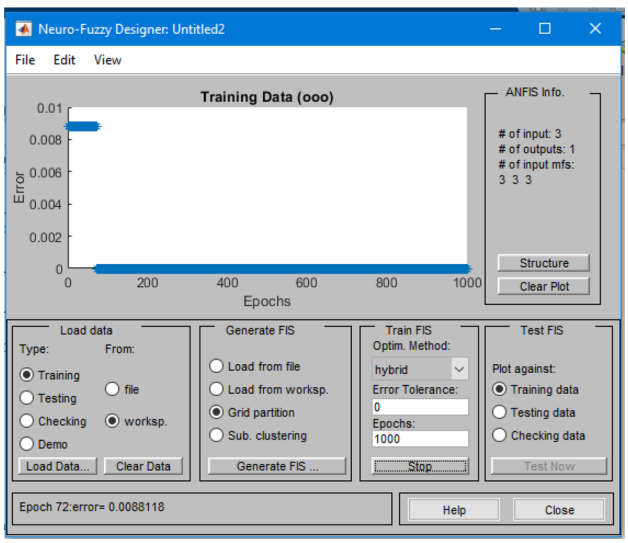

Fig. 7 Error minimization process of ANFIS

effective and better at predicting responses. Based on the statistical analysis, all of the approaches produced high-quality simulations due to their data fitting and prediction abilities.

Table 6 illustrate the prediction performance of the ANFIS, ANN, and RSM models for surface roughness, cutting force, and cutting temperature. The most approximate locations have a reduced failure rate; the differences between

Table 6 Predicted values by ANFIS, ANN and RSM

Number	Cutting condition	Predicted surface roughness (Ra)			Predicted cutting force (F)			Predicted cutting temperature (T)		
		ANFIS	ANN	RSM	ANFIS	ANN	RSM	ANFIS	ANN	RSM
1	HPC	0.854	0.86244	0.86	188	187.667	195.88	896.8	897.728	897.35
2	HPC	0.86	0.86128	0.86	162	162	174.63	891.9994	891.435	898.85
3	HPC	0.854	0.86244	0.86	188	187.667	195.88	896.8	897.728	897.35
4	HPC	0.89	0.89074	0.88	210	210.001	210.88	922.9986	922.016	916.98
5	HPC	0.68	0.68519	0.68	148	147.988	138.38	897.9971	897.593	896.73
6	HPC	1.03	1.0327	1.05	266	266.011	274.63	910.9993	912.855	917.23
7	HPC	1.12	1.1039	1.09	274	273.997	253.38	898.0004	898.096	897.98
8	HPC	0.71	0.70735	0.71	129	129.005	117.13	892.0015	892.675	890.48
9	HPC	0.81	0.80892	0.8	219	219.688	217.13	935.9992	929.395	924.35
10	HPC	0.85	0.85324	0.85	223	223.006	232.13	910.9998	912.642	923.23
11	HPC	0.854	0.86244	0.86	188	187.667	195.88	896.8	897.728	897.35
12	HPC	0.81	0.81352	0.83	154	154.001	159.63	865.9994	859.788	858.48
13	HPC	1.1	1.0949	1.1	308	307.451	289.63	922.9977	930.099	916.1
14	HPC	0.69	0.68755	0.68	111	111.383	102.13	847.999	854.449	850.1
15	HPC	0.81	0.81073	0.79	186	185.994	180.88	873.0003	871.826	877.73
16	HPC	0.854	0.86244	0.86	188	187.667	195.88	896.8	897.728	897.35
17	HPC	0.854	0.86244	0.86	188	187.667	195.88	896.8	897.728	897.35
18	Dry	1.004	1.00441836	1.02	237	237.34	237.76	967.1998	969.474	963.59
19	Dry	1.01	1.01534335	1.06	175	175.002	170.64	979.999	980.289	976.96
20	Dry	1.004	1.00441836	1.02	237	237.34	237.76	967.1998	969.474	963.59
21	Dry	1.12	1.0936854	1.09	253	253.004	257.26	991.999	995.476	1000.46
22	Dry	0.98	0.98017051	0.98	267	266.996	264.89	947.9991	949.059	950.21
23	Dry	1.35	1.31583045	1.31	389	388.334	380.14	998.999	995.53	1000.71
24	Dry	1.06	1.05162935	0.99	170	169.996	171.89	935.9991	935.408	940.09
25	Dry	0.78	0.80543241	0.8	135	135.118	134.14	966.999	966.183	963.34
26	Dry	1.004	1.00441836	1.02	237	237.34	237.76	967.1998	969.474	963.59
27	Dry	0.77	0.76092591	0.76	187.999	187.996	185.51	954.999	954.208	949.96
28	Dry	0.72	0.74647365	0.73	133	138.725	135.39	922.9991	921.979	926.46
29	Dry	1.06	1.03917986	1.05	304.999	305.011	308.64	979.999	980.382	987.09
30	Dry	1.28	1.27605494	1.28	292	292.008	293.51	973.999	974.753	977.21
31	Dry	0.96	0.95876816	0.94	220	219.992	214.76	916.9991	921.891	926.71
32	Dry	1.004	1.00441836	1.02	237	237.34	237.76	967.1998	969.474	963.59
33	Dry	1.18	1.19084393	1.24	330	330.002	336.39	973.999	972.19	963.84
34	Dry	1.004	1.00441836	1.02	237	237.34	237.76	967.1998	969.474	963.59

projected and experimental data are fewer for ANFIS models than for RSM and ANN models. ANN models, on the other hand, outperform RSM models. The obtained R^2 for surface roughness ANFIS models is 0.9947 (under HPC) and 0.9896 (under dry), while their values for ANN models are 0.9867 (under HPC) and 0.9837 (under dry). This can also demonstrate the capabilities of ANFIS models, which also show smaller residuals in Ra, F, and T (at various cutting conditions) as compared to ANN and RSM models. Furthermore, the RMSE and MAE values in Table 8 demonstrate that ANFIS models outperformed ANN and RSM models in terms of prediction capabilities for the evaluated material and process. According to the arguments presented above, ANFIS outperforms ANN and RSM in predicting surface roughness, cutting temperature, and cutting force under HPC and Dry cutting circumstances.

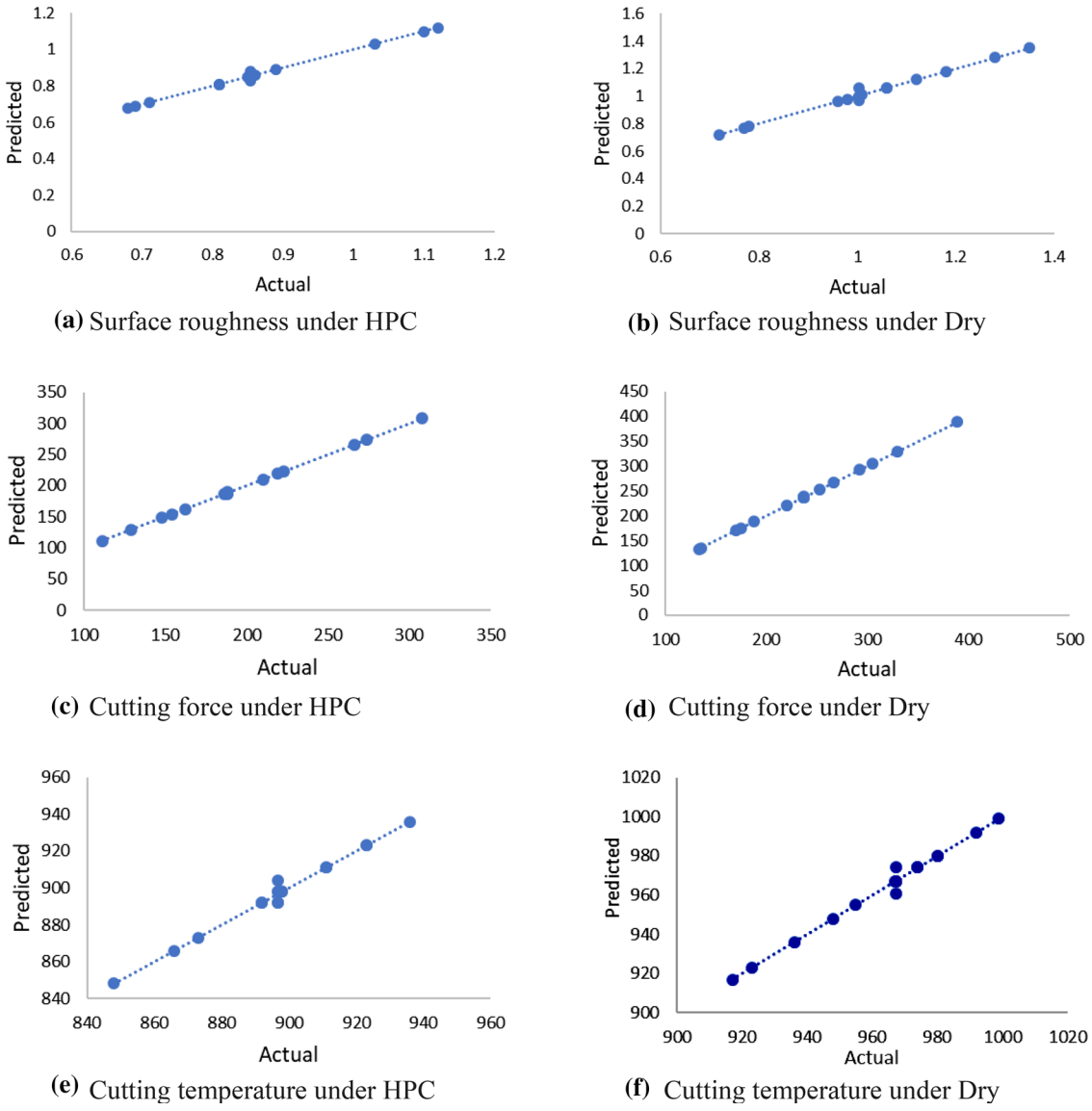

Fig. 8 **a** Surface roughness under HPC **b** Surface roughness under Dry **c** Cutting force under HPC **d** Cutting force under Dry **e** Cutting temperature under HPC **f** Cutting temperature under Dry

Table 7 R and R-squared values of ANFIS, ANN and RSM

Responses	Cutting condition	ANFIS predicted data		ANN predicted DATA		RSM predicted data	
		R	R-square	R	R-square	R	R-square
Surface roughness	HPC	0.997346	0.9947	0.99333	0.9867	0.991615	0.9833
	Dry	0.994786	0.9896	0.99182	0.9837	0.976883	0.9543
Cutting force	HPC	1	1	0.9993	0.9986	0.978928	0.9583
	Dry	1	1	0.9998	0.9996	0.998449	0.9969
Cutting temperature	HPC	0.993126	0.9863	0.98194	0.9642	0.955196	0.9124
	Dry	0.994585	0.9892	0.99015	0.9804	0.963483	0.9283

Table 8 RMSE, MAE values of ANFIS, ANN and RSM

Responses	Cutting condition	ANFIS predicted data		ANN predicted data		RSM predicted data	
		RMSE	MAE	RMSE	MAE	RMSE	MAE
Surface roughness	HPC	0.008812	0.05851	0.0143	0.82592	0.015146	1.27095
	Dry	0.016306	0.647195	0.02233	1.69319	0.034641	1.173574
Cutting force	HPC	0.342997	0.05882	0.45221	0.1444621	10.19448	4.76247
	Dry	0.342997	0.06266	1.45141	0.34462	3.638359	1.17357
Cutting temperature	HPC	2.435039	0.12596	4.0501	0.34184	6.157018	0.55827
	Dry	2.233436	0.0827355	3.13024	0.24292	5.760722	0.519803

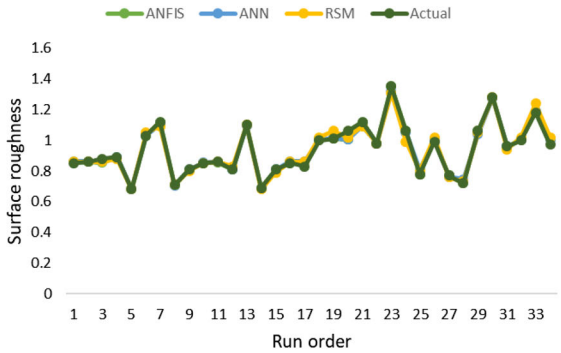

(a) Comparison of Actual (Ra) with predicted ANN, RSM and ANFIS predicted (Ra)

(b) Comparison of Actual (F) with predicted ANN, RSM and ANFIS predicted (F)

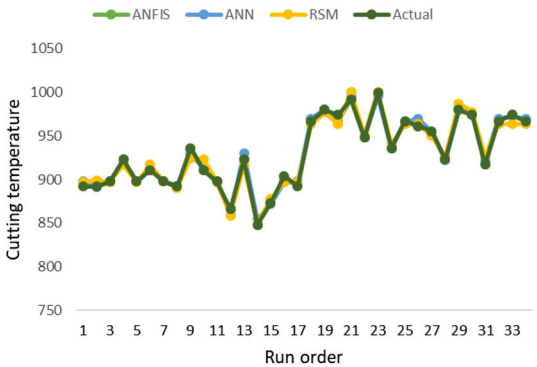

(c) Comparison of Actual (T) with predicted ANN, RSM and ANFIS predicted (T)

Fig. 9 **a** Comparison of Actual (Ra) with predicted ANN, RSM and ANFIS predicted (Ra) **b** Comparison of Actual (F) with predicted ANN, RSM and ANFIS predicted (F) **c** Comparison of Actual (T) with predicted ANN, RSM and ANFIS predicted (T)

3.5 Comparison with recent works

A detailed comparative analysis between the proposed ANFIS framework with the previous works on predicting machining response in hard turning process has been presented in this section. In [19] Surface roughness and cutting force under dry condition was predicted using ANN and RSM model.The final R-Squared value for surface roughness and cutting force were 0.9679 and 0.9980 respectivley. In another paper, surface roughness was predicted using ANFIS Model and the R-squared value was 0.9801 [43]. Cutting gemperature was predicted by ANN and ANFIS under dry conditions and the final R-squared values were 0.8978 and 0.9594 respectivley [28] in another article.

In [19] prediction was only made in dry conditions, also the predictive accuracy was significantly lower than the proposed ANFIS model which was 0.9896 and 1 for surface roughness and cutting force respoectively. In [43] the prediction was made for only two output parameter which narrowed the scope of that model; wherease the proposed model was prepared for 6 output parameters, which made our model more generic. In[28] the prediction was only made for one response under one condition and the accuracy was also lower than the proposed ANFIS Model in this work.From this analysis, it can be showed that the proposed ANFIS Model imparts significant improvement over the exsting works on hard turning process under Dry and HPC conditions.

4 Conclusion

Using ANFIS, RSM, and ANN, the researchers investigated the effects of varying cutting conditions on surface roughness, cutting temperature, and cutting force by varying cutting speeds, depth of cut, and feed rates. The following are some key takeaways from the discussion just above about how things turned out:

- The cutting speed, feed rate, and depth of cut are all statistically significant. Because of the larger F-value, the feed rate is the most important factor in determining surface roughness and depth of cut for cutting force.
- In addition to improving the surface quality, high-pressure coolant also provides a low surface roughness, which allows for the attainment of the required precision. When compared to dry cutting conditions, it also lowers the cutting temperature and cutting force.
- As a modeling technique, the response surface methodology can help uncover unimportant major factors, interactions, or unimportant quadratic terms in the model, reducing the problem's overall complexity.
- Findings from simulations of the analyzed properties using ANFIS,ANN and RSM models based on real data showed that each model can produce correct results.
- ANN and RSM were shown to be inferior in prediction when compared to ANFIS models, which had a larger and better determination coefficient (R^2) (close to 1).Additionally, RMSE, MSE, and MAPE were used to verify this, as these parameters had lower values in ANFIS than RSM and ANN.

Acknowledgements The authors would like to thank Directorate of Advisory Extension and Research Services (DAERS), BUET, Dhaka, Bangladesh, for providing the laboratory facility to carry out the research work. This research did not receive any specific grant from funding agencies in the public, commercial, or not-for-profit sectors.

Funding This study did not receive any grant from any of funding agencies.

Declarations

Conflict of interest The authors declare that they have no conflict of interest.

Appendix

See Figs. 10, 11, 12, 13, 14

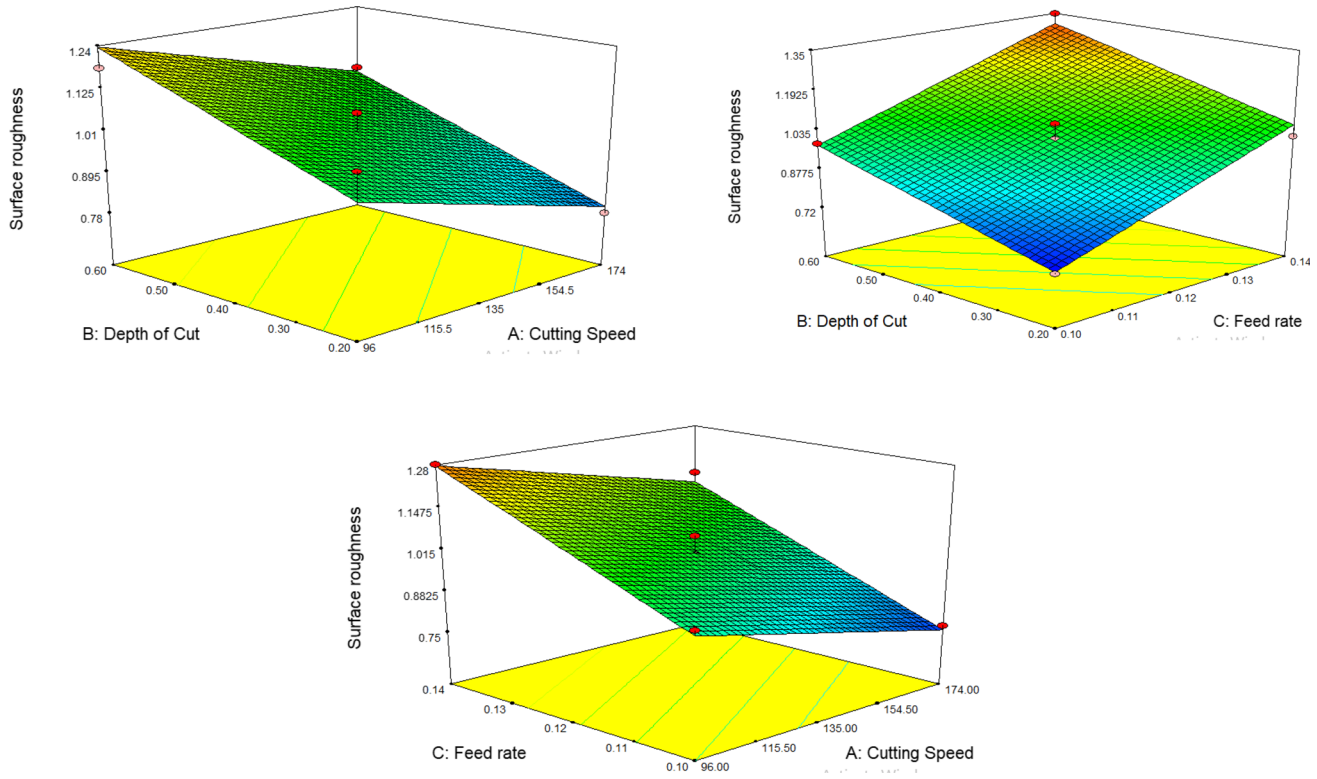

Fig. 10 Response Surface plot of Surface roughness under Dry

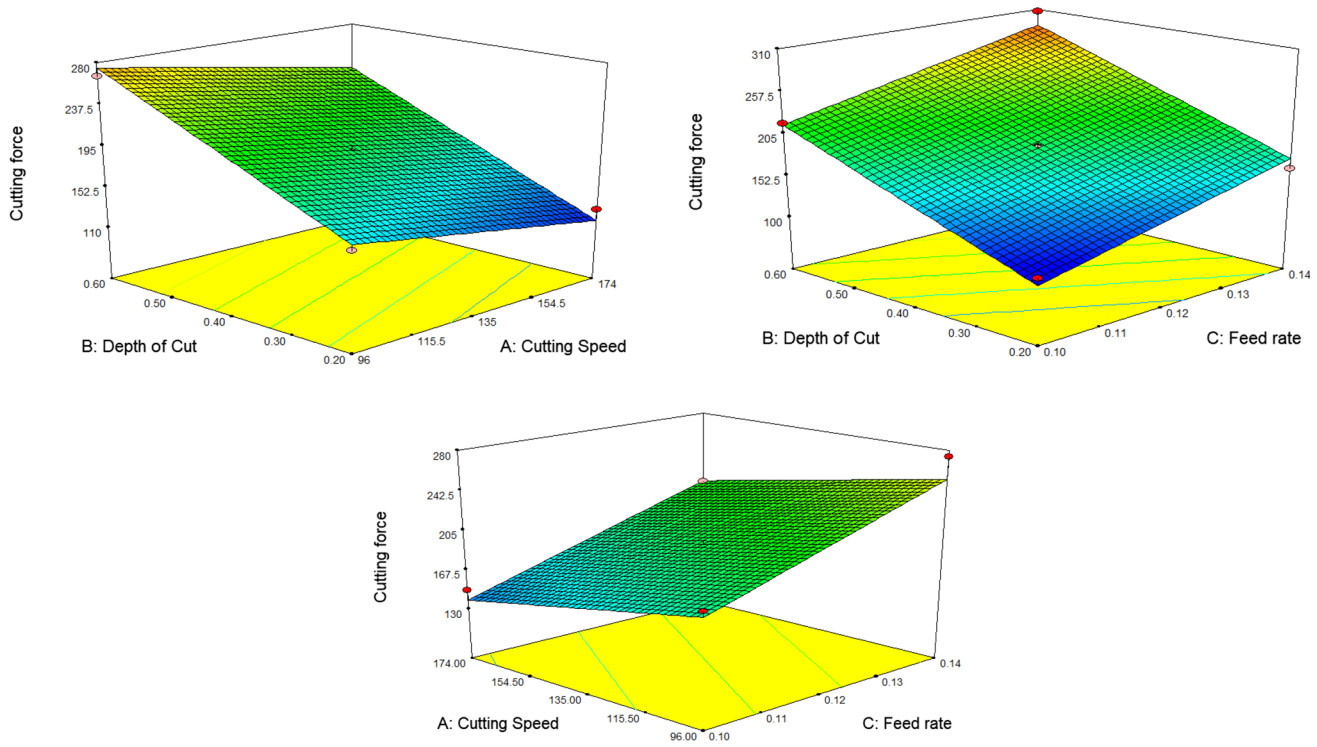

Fig. 11 Response Surface plot of Cutting force under HPC

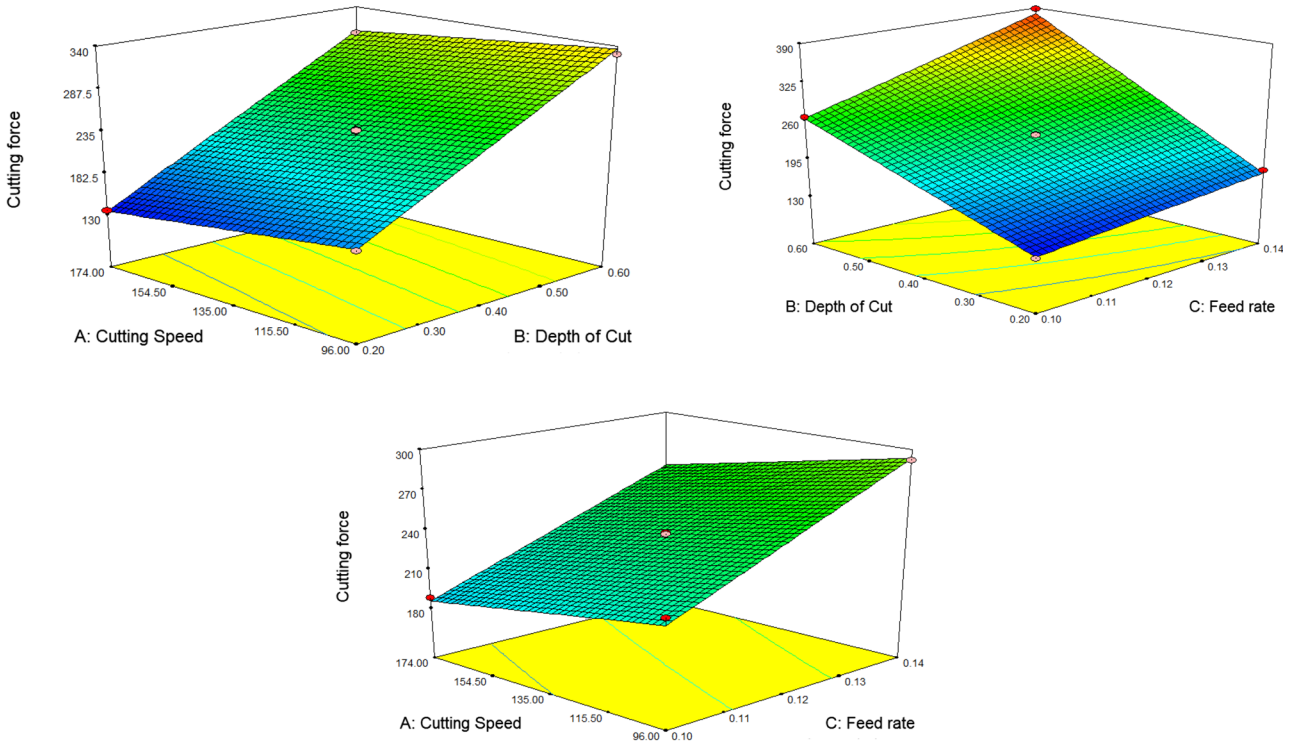

Fig. 12 Response Surface plot of Cutting force under Dry

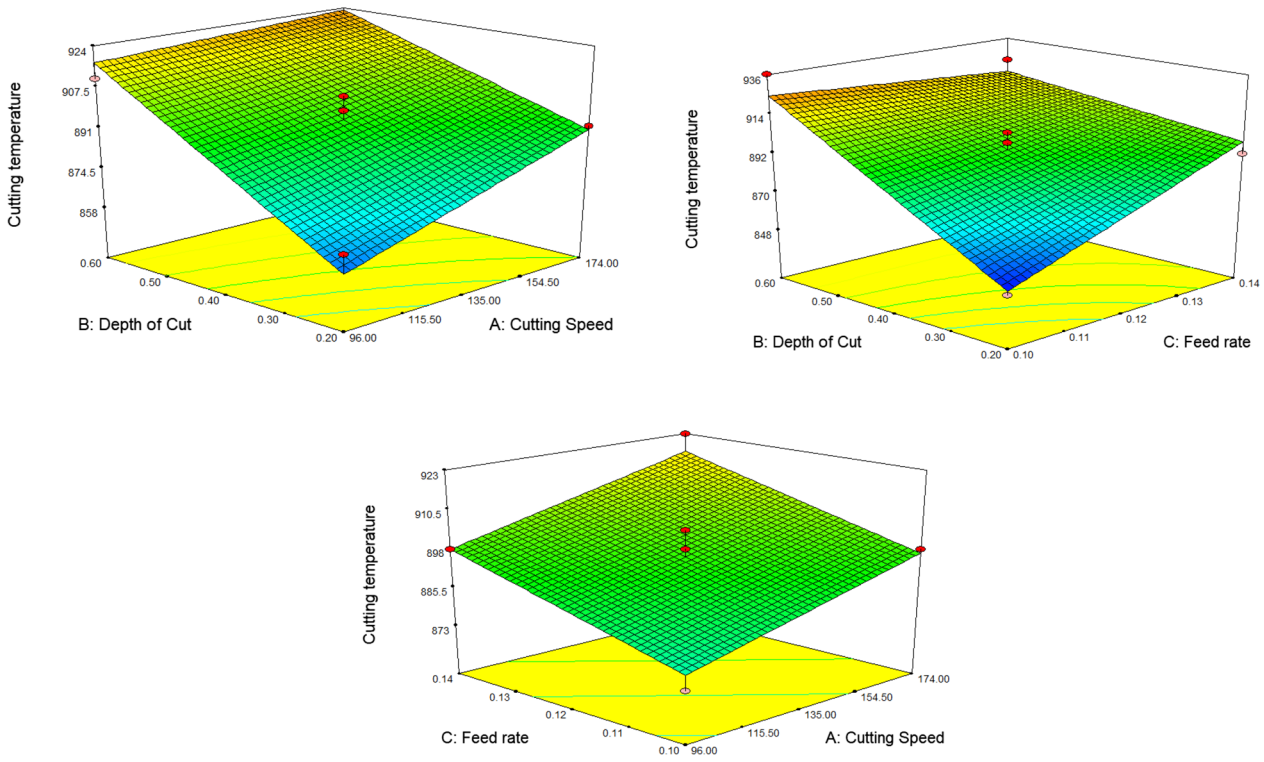

Fig. 13 Response Surface plot of Cutting temperature under HPC

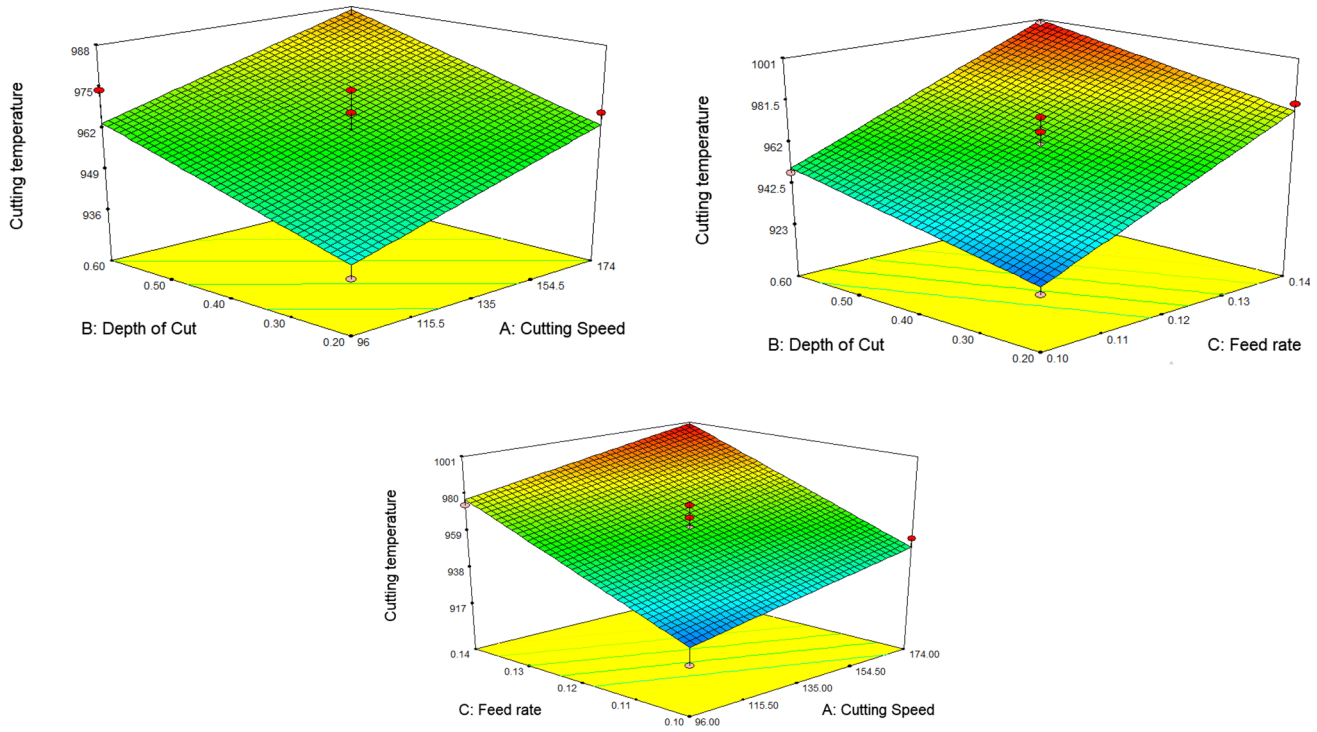

Fig. 14 Response Surface plot of Cutting temperature under Dry

References

1. König, W., Berktold, A., Koch, K.-F.: Turning versus grinding–a comparison of surface integrity aspects and attainable accuracies. CIRP Ann. **42**, 39–43 (1993)
2. Özel, T., Karpat, Y.: Predictive modeling of surface roughness and tool wear in hard turning using regression and neural networks. Int. J. Mach. Tools Manuf. **45**, 467–479 (2005)
3. Naragund, V.S., Panda, P.K.: Electrospinning of cellulose acetate nanofiber membrane using methyl ethyl ketone and N, N-Dimethylacetamide as solvents. Mater. Chem. Phys. (2020). https://doi.org/10.1016/j.matchemphys.2019.122147
4. Mia, M., Dhar, N.R.: Effect of high pressure coolant jet on cutting temperature, tool wear and surface finish in turning hardened (HRC 48) steel. J. Mech. Eng. **45**, 1–6 (2015)
5. Naves, V.T.G., Da Silva, M.B., Da Silva, F.J.: Evaluation of the effect of application of cutting fluid at high pressure on tool wear during turning operation of AISI 316 austenitic stainless steel. Wear **302**, 1201–1208 (2013)
6. Bouacha, K., Yallese, M.A., Mabrouki, T., Rigal, J.F.: Statistical analysis of surface roughness and cutting forces using response surface methodology in hard turning of AISI 52100 bearing steel with CBN tool. Int. J. Refract. Met. Hard Mater. **28**, 349–361 (2010). https://doi.org/10.1016/j.ijrmhm.2009.11.011
7. Shihab, S.K., Khan, Z.A., Mohammad, A., Siddiqueed, A.N.: RSM based study of cutting temperature during hard turning with multilayer coated carbide insert. Procedia Mater. Sci. **6**, 1233–1242 (2014)
8. Mohsan, A.U.I.H., Liu, Z., Padhy, G.K.: A review on the progress towards improvement in surface integrity of Inconel 718 under high pressure and flood cooling conditions. Int. J. Adv. Manuf. Technol. **91**, 107–125 (2017)
9. Ezugwu, E.O., Bonney, J.: Finish machining of nickel-base Inconel 718 alloy with coated carbide tool under conventional and high-pressure coolant supplies. Tribol. Trans. **48**, 76–81 (2005)
10. Das, A., Mukhopadhyay, A., Patel, S.K., Biswal, B.B.: Comparative assessment on machinability aspects of AISI 4340 alloy steel using uncoated carbide and coated cermet inserts during hard turning. Arab. J. Sci. Eng. **41**, 4531–4552 (2016). https://doi.org/10.1007/s13369-016-2160-0
11. Sahoo, A.K., Sahoo, B.: Performance studies of multilayer hard surface coatings (TiN/TiCN/Al_2O_3/TiN) of indexable carbide inserts in hard machining: Part-II (RSM, grey relational and techno economical approach). Meas. J. Int. Meas. Confed. **46**, 2868–2884 (2013). https://doi.org/10.1016/j.measurement.2012.09.023
12. Mital, A., Mehta, M.: Surface finish prediction models for fine turning. Int. J. Prod. Res. **26**, 1861–1876 (1988)
13. Courbon, C., Kramar, D., Krajnik, P., Pusavec, F., Rech, J., Kopac, J.: Investigation of machining performance in high-pressure jet assisted turning of Inconel 718: an experimental study. Int. J. Mach. Tools Manuf. **49**, 1114–1125 (2009)
14. Sultana, I., Dhar, N.R.: Performance of Coated Carbide Insert for High Speed Machining of Hardened Steel under High Pressure Coolant (HPC) Condition, Prod. Eng. (2010).
15. Sharma, V.S., Dhiman, S., Sehgal, R., Sharma, S.K.: Estimation of cutting forces and surface roughness for hard turning using neural networks. J. Intell. Manuf. **19**, 473–483 (2008)
16. Mia, M., Dhar, N.R.: Prediction of surface roughness in hard turning under high pressure coolant using artificial neural network. Measurement **92**, 464–474 (2016)
17. Mia, M., Dhar, N.R.: Modeling of surface roughness using RSM, FL and SA in dry hard turning. Arab. J. Sci. Eng. **43**, 1125–1136 (2018)
18. Lakhdar, B., Athmane, Y.M., Salim, B., Haddad, A.: Modelling and optimization of machining parameters during hardened steel

AISID3 turning using RSM, ANN and DFA techniques: comparative study. J. Mech. Eng. Sci. **14**, 6835–6847 (2020)
19. Zerti, A., Yallese, M.A., Zerti, O., Nouioua, M., Khettabi, R.: Prediction of machining performance using RSM and ANN models in hard turning of martensitic stainless steel AISI 420. Proc Inst Mech Eng Part C J Mech Eng Sci **233**, 4439–4462 (2019)
20. Mia, M., Dhar, N.R.: Response surface and neural network based predictive models of cutting temperature in hard turning. J. Adv. Res. **7**, 1035–1044 (2016)
21. Labidi, A., Tebassi, H., Belhadi, S., Khettabi, R., Yallese, M.A.: Cutting conditions modeling and optimization in hard turning using RSM, ANN and desirability function. J. Fail. Anal. Prev. **18**, 1017–1033 (2018)
22. Mia, M., Khan, M.A., Dhar, N.R.: Study of surface roughness and cutting forces using ANN, RSM, and ANOVA in turning of Ti-6Al-4V under cryogenic jets applied at flank and rake faces of coated WC tool. Int. J. Adv. Manuf. Technol. **93**, 975–991 (2017)
23. Lo, S.-P.: The application of an ANFIS and grey system method in turning tool-failure detection. Int. J. Adv. Manuf. Technol. **19**, 564–572 (2002)
24. Kumar, S., Singh, B.: Chatter prediction using merged wavelet denoising and ANFIS. Soft Comput. **23**, 4439–4458 (2019)
25. Rizal, M., Ghani, J.A., Nuawi, M.Z., Haron, C.H.C.: Online tool wear prediction system in the turning process using an adaptive neuro-fuzzy inference system. Appl. Soft Comput. **13**, 1960–1968 (2013)
26. Ho, W.-H., Tsai, J.-T., Lin, B.-T., Chou, J.-H.: Adaptive network-based fuzzy inference system for prediction of surface roughness in end milling process using hybrid Taguchi-genetic learning algorithm. Expert Syst. Appl. **36**, 3216–3222 (2009)
27. Savkovic, B., Kovac, P., Dudic, B., Rodic, D., Taric, M., Gregus, M.: Application of an adaptive "neuro-fuzzy" inference system in modeling cutting temperature during hard turning. Appl. Sci. (2019). https://doi.org/10.3390/app9183739
28. Sredanovic, B., Cica, D.: Comparative study of ANN and ANFIS prediction models for turning process in different cooling and lubricating conditions. SAE Int. J. Mater. Manuf. **8**, 586–591 (2015)
29. Jamli, M.R., Fonna, S.: Comparison of adaptive neuro fuzzy inference system and response surface method in prediction of hard turning output responses. J. Adv. Manuf. Tech. **12**, 153–164 (2018)
30. Zaman, P.B., Saha, S., Dhar, N.R.: Hybrid Taguchi-GRA-PCA approach for multi-response optimisation of turning process parameters under HPC condition. Int. J. Mach. Mach. Mater. **22**, 281–308 (2020). https://doi.org/10.1504/IJMMM.2020.107059
31. Nagata, Y., Chu, K.H.: Optimization of a fermentation medium using neural networks and genetic algorithms. Biotech. Lett. **25**, 1837–1842 (2003)
32. Tebassi, H., Yallese, M.A., Meddour, I., Girardin, F., Mabrouki, T.: On the modeling of surface roughness and cutting force when turning of Inconel 718 using artificial neural network and response surface methodology: accuracy and benefit, Period. Polytech Mech. Eng. **61**, 1–11 (2017)
33. Valluru, R., Hayagriva, R.: C++ neural networks and fuzzy logic, (1996).
34. Karayiannis, N., Venetsanopoulos, A.N.: Artificial neural networks: learning algorithms, performance evaluation, and applications. Springer, Berlin (1992)
35. Myers, R.H., Montgomery, D.C., Anderson-Cook, C.M.: Response surface methodology: process and product optimization using designed experiments. Wiley, New Jersey (2016)
36. Draper, N.R., Smith, H., Pownell, E.: Applied regression analysis [Google Sch], vol. 3. Wiley, New York, NY (1966)
37. Miroslav, R.: Optimizing cutting parameters based on cutting force in tube turning using taguchi method. Rev. Tehnol. Neconv. **16**, 29 (2012)
38. Bui, V.T., Hoang, T.T., Duong, T.L., Truong, D.N.: Dynamic voltage stability enhancement of a grid-connected wind power system by ANFIS controlled static var compensator, International conference on system science and engineering IEEE, pp 174–177 (2019)
39. Cuevas, E., Gálvez, J., Avalos, O.: Gravitational search algorithm for non-linear system identification using ANFIS-Hammerstein approach. In: Recent metaheuristics algorithms param. identif., pp. 97–134. Springer, Berlin (2020)
40. Jang, J.-S., Sun, C.-T.: Neuro-fuzzy modeling and control. Proc. IEEE. **83**, 378–406 (1995)
41. Basheer, A.C., Dabade, U.A., Joshi, S.S., Bhanuprasad, V.V., Gadre, V.M.: Modeling of surface roughness in precision machining of metal matrix composites using ANN. J. Mater. Process. Tech. **197**, 439–444 (2008)
42. Schober, P., Boer, C., Schwarte, L.A.: Correlation coefficients: appropriate use and interpretation. Anesth. Analg. **126**, 1763–1768 (2018)
43. Shivakoti, I., Kibria, G., Pradhan, P.M., Pradhan, B.B., Sharma, A.: ANFIS based prediction and parametric analysis during turning operation of stainless steel 202. Mater. Manuf. Process. **34**, 112–121 (2019). https://doi.org/10.1080/10426914.2018.1512134